Deformation Monitoring and Prediction of Open-pit Mine Slope Based on GBInSAR Technology and LSTM Neural Network

Miao Li [1*], Keliang Ding [1], Lei Pang [1], Ya Shu [1], Yanhui Qu [1]

[1] School of Geomatics and Urban Spatial Informatics, Beijing University of Civil Engineering and Architecture, Beijing, 102627, China - limiao010220@163.com

Keywords: GBInSAR, LSTM model, Open-pit Mine Slope, Deformation Monitoring, Prediction.

Abstract

High-precision and real-time deformation monitoring of open-pit mine slopes provides reliable data support for slope safety early warning and governance, which is directly related to the production efficiency of open-pit mines and the safety of personnel and property. Compared with traditional measurement technologies, Ground-Based Synthetic Aperture Radar Interferometry (GBInSAR), as a novel deformation monitoring technology developed in the past two decades, possesses significant advantages including all-weather operation, all-time coverage, large-scale monitoring, non-contact measurement, high precision, and real-time observation. It has become one of the core technical equipment for monitoring dangerous slopes in open-pit mines and is widely applied in open-pit mine slope safety monitoring scenarios. Against this background, how to effectively integrate ground-based InSAR data with advanced prediction models to enhance the early prediction capability of slope deformation has become a crucial research direction in this field. To address this issue, this paper proposes a GBInSAR time-series data processing method based on the Long Short-Term Memory (LSTM) model. Firstly, the initial deformation information of a slope is extracted from the pre-monitoring data of the IBIS system, and then an LSTM-based slope deformation prediction model is constructed to achieve short-term accurate prediction of future deformation trends. By organically combining the LSTM model with ground-based InSAR data, this paper deeply explores the temporal evolution characteristics of slope deformation and establishes a slope deformation prediction model. This study aims to explore the application of ground-based InSAR in slope deformation monitoring based on the LSTM model; by constructing a slope deformation prediction model and a risk early warning mechanism, it provides effective technical support and decision-making basis for the safety management of open-pit mine slopes.

1. Introduction

Stability of slopes in the open-pit mines is a key assurance in the mine safety and normal functioning. Due to the mining activities of ore body, the geological stress distribution of the slope changes, whereby slope deformation as well as its long term and short term stability could be realized. Therefore, it is of significant importance how the deformation of the slope can be acquired correctly and a scientific and reasonable early warning system developed to reduce the risk of mine landslide disasters. The available slope deformation monitoring technologies are mostly composed of traditional contact monitoring (e.g., total stations, GNSS, leveling surveys) (Li et al., 2023) and sophisticated remote sensing monitoring technologies (Izumi et al., 2021). Their accuracy, however, is limited by certain factors including climate, time and visibility. GBInSAR represents one of the technologies that can be highly beneficial as a complement to the space-borne synthetic aperture radar interferometry (InSAR) technology (Xiao et al., 2021; Chen et al., 2024; Zhang and Zhou, 2024). Not only does it have the best observation positions and constant performance of observation but has such advantages as flexibility and variability, high resolution, stable platforms, short observation cycles, and relatively low costs (Cui et al., 2024). The GBInSAR being a non-contact type of measurement is suitable in real-time measurements of dangerous slopes deformation. In different weather conditions, GBInSAR is capable of delivering accuracy of sub-millimeter level in large-scale deformations, achieves continuous dynamic monitoring of the slope, and has extensive data support of slope stability analysis(Han et al., 2022). However, despite the fact that the data provided by GBInSAR on deformation can determine the dynamics of the slope, there is some delay in early warning used on the basis of monitoring data, and it is not easy to observe possible trends of instability in time (Izumi et al., 2020). Thus, to further improve the foresight and precision of early warning systems, there is a necessity to combine deep learning prediction models to perform trend extrapolation on the deformation data. This also illustrates why the LSTM-based GBInSAR time-series processing model presented in this paper is needed, i.e., using the powerful side of learning the temporal features of the LSTM models, which is the capacity of strong learning, to extract the inherent correlation of GBInSAR-monitored deformation data with time, it can effectively offset the laggardiness of the pure monitoring data and offer more timely and reliable technical assistance in early warning of slope instability risk (Zhou et al., 2014). This form of combined strategy does not only open the maximum extent of application value of GBInSAR to slope monitoring, but also encourages the enhancement of open-pit mine slope safety management by turning it into a pre-warning form instead of post-monitoring, which has significant practical value to the maintenance of safety in mine production and minimization of the losses incurred by landslides.

According to current studies, slope deformation characteristic prediction is mainly done based on surface deformation measurements obtained through conventional ground based observations. As an example, the Baishuihe Landslide in the Three Gorges Reservoir Area was chosen as the object of the study by Liu et al. (2023), where the monitoring of GPS displacement was used along with a PSO-SVR coupling model to predict displacement. The findings showed that the estimation outcomes were close to the actual trends of displacement variations, which confirmed the efficiency of the given conventional data-driven prediction technique. Regarding the development of monitoring technologies, such Italian scholars like Tarchi D. investigated a ground-based SAR system and compared its monitoring outputs with other traditional

This contribution has been peer-reviewed. The double-blind peer-review was conducted on the basis of the full paper.
https://doi.org/10.5194/isprs-annals-X-3-W3-2025-173-2026

methods of monitoring, thus confirming the possibility of ground-based SAR systems implementation to slope deformation monitoring (Zou et al., 2023). A ground-based SAR system was used by Noferini L. in 2007 in monitoring landslides in Karawanken Alps (note: geographical accuracy should be Karina Alps) was used. Noferini L. was able to examine the accuracy of Lean ground-based SAR systems by correlating the accuracy with the findings of the GPS monitoring. As well, Luzi G. had performed monitoring of the Alpine glacier displacement by means of Ground-Based SAR (GB-SAR) and the experimental outcomes showed that GB-SAR technology was capable of detecting the small-scale displacement changes of the glaciers and hence validated the application of the technology in non-slopes cases like glacier monitoring. Ground-based SAR deformation monitoring technology was also presented as a part of the deformation simulation of building during an earthquake (Dai et al., 2022), which demonstrated the fact that it was feasible in detecting building deformations outside the frames of geotechnical engineering (Gong et al., 2024). As the new information technologies continue to be developed like artificial intelligence, machine learning and nonlinear prediction models are widely used in predicting deformation of landslides. Xu et al. (2025) used the case of the Fanqian Landslide in the Three Gorges Reservoir Area as an example to carry out surface deformation monitoring research by using SBAS-InSAR time-series data with the LSTM model. It has been shown that the correlation coefficients of the prediction performance of the LSTM were 0.9455 and 0.9829 and were much higher than in Back Propagation (BP) neural network model and the Support Vector Machine (SVM) model. This demonstrates the excellence of deep learning models such as LSTM in time-series deformation input activities. Moreover, Chang et al. (2022) used the Squeeze-and-Excitation Capsule Network (SE-CapNet) architecture to estimate the likelihood of landslides in the Yichang Region of the Yangtze River Basin and found that the landside detection accuracy of this architecture in the region conducted 96.29, which is useful information in integrating advanced neural network designs in geohazard analysis.

All of these studies prove that slope deformation monitoring has shifted towards more complex non-contact technologies and more innovative approaches to slope deformation prediction, verification, or intelligence-driven deep learning methods have been developed (Yang et al., 2022). Nevertheless, it is still necessary to optimize better the combination of high-precision GBInSAR time-series data with potent deep-learning models (including LSTM) further, which is one gap to be filled by the proposed study in the given paper. This study aims to address this existing research gap through the visualization of the synergy between high-quality monitoring data offered by GBInSAR and strong temporal feature extraction capabilities of LSTM thus contributing to the practical use of integrated monitoring-prediction system in the operation of mine safety (Lv et al., 2024).

In the recent past as the world keeps enhancing the concept of artificial intelligence and the deployment of deep learning technology, data-based methods have displayed enormous application prospects in the prediction of slope deformation. One of these approaches is the LSTM network, a deep learning model that can be used to analyze time series data, so it can thoroughly address the time dynamics of the monitoring information (Ma & Lu, 2023). The model can be trained on the historical values of deformation using the GBInSAR monitoring, but through this, a slope deformation prediction system can be formed, and, consequently, the future trends of the deformation can be predicted accurately within a short period.

To sum up, the proposed solution of using GBInSAR technology and the LSTM prediction model is a new method of slope deformation monitoring and early alert in open pit mines. The paper aims to discuss the hybrid use of GBInSAR and LSTM, and develop intelligent early warning algorithm with deep learning. It is aimed at enhancing quality and timeliness of slope monitoring and early warning in the open-pit mines, and offer theoretical support and technical certification of mine safety management.

2. LSTM Model

The LSTM network is a particular version of RNN model. The hypothesis was first introduced by Sepp Hochreiter and Jurgen Schmidhuber in 1997. This model is aimed at resolving the problems of gradient decay and gradient explosion in conventional RNN when utilizing long sequences training (Chai et al., 2021). As Figure 1 shows, it implies that LSTM is not seemingly similar to RNN. In order to improve the memory and expression functions (storage and transmission of information) of RNN, LSTM introduces three gating dynamics and a cell state that allow the model to autonomously determine which information should be maintained and which should be forgotten in order to better represent the long-term dependencies in the sequence (Zhang et al., 2025).

The basic structure of LSTM includes a recurrent unit and three gating units: the input gate, the forget gate, and the output gate. The recurrent unit takes the current input and the previous output as inputs, and outputs the current output and passes it to the next state. The input gate controls the influence of the current input on the state, the forget gate controls the influence of the previous state on the current state, and the output gate controls the influence of the current state on the output (Chataoui, 2024). The memory unit is used to store and transmit long-term information. Based on this, LSTM has long-term memory capabilities and the characteristic of preventing gradient disappearance, so this paper selects LSTM as the training basis for the inventory prediction model.

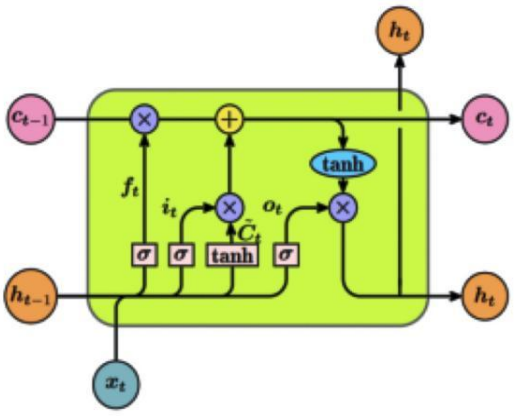

Figure 1. LSTM model cell structure.

Among them, the calculation formulas for the input gate, the forget gate and the output gate are as follows:

$$\begin{aligned} i_t &= \sigma(W_i \cdot [h_{t-1}, x_t] + b_i) \\ f_t &= \sigma\big(W_f \cdot [h_{t-1}, x_t] + b_f\big) \\ o_t &= \sigma(W_o \cdot [h_{t-1}, x_t] + b_o) \end{aligned} \quad (1)$$

3. Study Area and Data

3.1 Study Area

The experimental object is a certain open-pit mine slope in Xilinhot City, Xilingol League, Inner Mongolia Autonomous Region. The mine is located 6 kilometers north of Xilinhot City, Inner Mongolia, with geographical coordinates of 116° 00′ 05.26" east longitude and 43° 59′ 02.29" north latitude. The overall shape is a north-east to south-west (NE-SW) strip, with asymmetrical wide gentle anticlines on both sides. This open-pit mining area slope is a typical rock slope, with a large height difference of the slope, a steep slope, and the mining area has smog, dust, and poor visibility. As this open-pit coal mine continues to expand and extend, the stability of the southern slope has become an important factor restricting its safe production (Yin et al., 2024). Therefore, real-time monitoring of the slope stability is required.

Figure 2. Mine area.

The study area of this article is the middle part of the southern slope, which is in a stepped shape, as shown in Figure 3. The IBIS system used in this experiment was installed in a stable area opposite to the monitoring slope, at a distance of 1600 meters from the monitoring slope (Huang et al., 2019). It was equipped with a radar, a linear track, a laptop computer and a power supply. The location of the radar provided good visibility for the monitoring area, ensuring that the entire slope could be monitored. This computer software is used for real-time monitoring of slope deformation (Chen et al., 2023).

(a) (b)

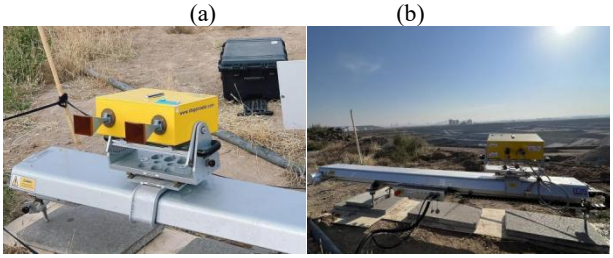

(c) (d)

(e) (f)

Figure 3. (a) Full view of the slope; (b) Experimental area of the slope and the layout of the IBIS-L; (c) IBIS-L sensor; (d) Linear Scanner; (e) Power supply module; (f) Control and acquisition notebook.

3.2 Experimental Result

The key parameters measured during this process are illustrated in Table 1:

Parameter	Value
Measuring distance range	700~1600m
Rail length	2m
Band	Ku Band
Range resolution	0.75m
Azimuthal resolution	4.38mrad
Time interval between two images	6min
Time	78h

Table 1. SAR data acquisition parameters

This experiment was conducted from 08:21 on October 15, 2024 to 15:01 on October 18, 2024 (China Standard Time), using the GBInSAR technology for monitoring. During the 4 day monitoring period, a total of 436 images were obtained. As shown in the figure, at several points on the slope, the deformation amplitude reached -5mm to 5mm during the experiment. Based on the three parameter indicators of thermal signal-to-noise ratio, estimated signal-to-noise ratio, and correlation, three high-quality deformation points were selected. After data processing, the cumulative deformation amplitudes of the experimental area were obtained. To further analyze the deformation trend of the slope body, characteristic points P1, P2, and P3 were selected in the areas with significant deformation, as shown in Figure 6. The cumulative deformation amplitudes of P1, P2, and P3 were 135.3 mm, 114.2 mm, and 102.7 mm, respectively.

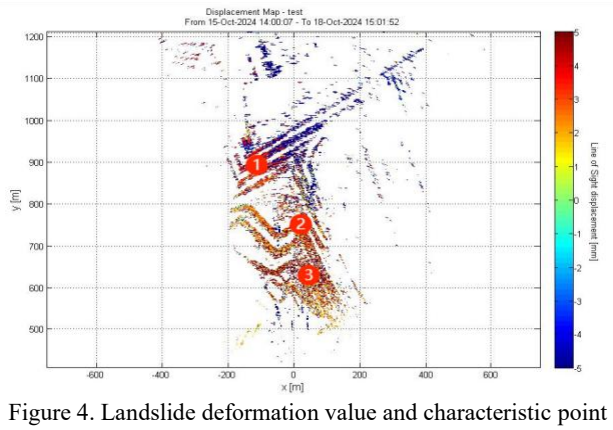

Figure 4. Landslide deformation value and characteristic point positions.

4. Deformation prediction

This paper proposes a GBInSAR slope deformation prediction method based on the LSTM model, aiming to enhance the deformation monitoring and prediction capabilities of open-pit mine slopes. The IBIS-L system is employed for real-time, high-precision displacement measurement on open-pit mine slopes, and the parameters of this system are optimized and adjusted to obtain the deformation data of each measurement point of the slope under the time series (Long et al., 2022). Subsequently, a deep learning sample library is constructed based on the pre-processed GB-InSAR deformation data set, and the LSTM model is trained based on this data set. Through hyperparameter optimization, the prediction accuracy and computational efficiency of the model are improved, thereby achieving accurate prediction of the future deformation trend of the slope. This provides scientific and reliable deformation warning support for open-pit mine slopes.

4.1 Data Normalization

To achieve a quicker convergence and make the predictions more precise, the interval between values fed to the neural network model must be kept even. The value scale of the variables should be adapted manually and adjusted to the scale. Techniques of common use are the following.

Normalization is the process of changing the value of the variables to the range between 0 and 1 or between -1 and 1. To compute first, the range of change of a given variable, the minimum value is deducted with the maximum value of the given variable. Thereafter, taking a single value in the variable of X, divide the value with the range of variable X then scale the value to an interval of 0 to 1; this procedure is known as maximum and minimum normalization expressed as the following equation:

$$X_{i(normalized)} = \frac{X_i - X_{min}}{X_{max} - X_{min}} \tag{2}$$

4.2 LSTM Network Design

Once the network architecture design has been completed, the training dataset could be inputted into the model to be trained. Training involves some complex structure in neural networks, therefore, the model is prone to overfitting with the increase in the number of iterations. A dropout layer is therefore incorporated to the LSTM module to improve the generalization ability of the model in addition to eliminating overfitting. The main purpose of this layer is to randomly switch off a good percentage of neurons in the LSTM layer every training step. It has been experimentally shown that additional layers to the LSTM do not produce any discernible increment in the predictive accuracy of the model. Also, the time step size is a very important parameter that should be chosen. To perform experiments in this paper, a time step size of 10 is used, implying that the deformation variable in the next time step is estimated using deformation data before 10 time steps (Song et al., 2020).

4.3 Hyperparameter Selection

The neural networks models have a huge number of hyper parameters that control the architecture, functionality, and efficiency of a model and therefore are key in producing high-accuracy results. The grid search technique was used as a hyperparameter search in this experiment. In particular, the search space of hyperparameters was determined, and the model performance was measured at a certain hyperparameter step to obtain the combination of the best combination of hyperparameters that produced the best model performance (Wu et al., 2019). Such an important aspect is the choice of the loss function that influences the level of prediction accuracy of the model (Ma and Lu, 2023). The evaluation indicators of model accuracy adopted in this research involved mean squared error (MSE) and mean absolute error (MAE), with their help the prediction performance of the model can be measured and be used to streamline the model and bestow the appropriate model.

MAE is a measure of the average size of errors in a predictive set of values by finding the absolute distance between the values predicted and the observed values. The primary benefits of MAE are that it does not take into consideration the orientation of these errors, now it can only speak of their size, based on the way as it can be calculated as the following:

$$MAE = \frac{1}{n}\sum_{i=1}^{n} |y_i - \hat{y}_i| \tag{3}$$

MSE usually refers to the formula for calculating the average value of the square of the difference between the predicted value and the actual observed value (Liu et al., 2025). The calculation method is as follows:

$$MSE = \frac{1}{n}\sum_{i=1}^{n} (y_i - \hat{y}_i)^2 \tag{4}$$

Among them, y_i is the true value (the target value); $\hat{y}_i$ is the predicted value; and n is the sample size.

As the model goes through its training phase, the fitting degree of the model is determined by calculating the size of the loss function. The model's efficacy is indicated by the eventual achievement of equivalent loss rates in the training and validation sets, which is indicative of a satisfactory fitting effect. The model hyperparameter combinations determined by the grid search method are shown in Table 2:

Hyperparameter Name	Value
LSTM_units	124
Batch_size	64
Epochs	800

Table 2. LSTM model hyperparameter combination table

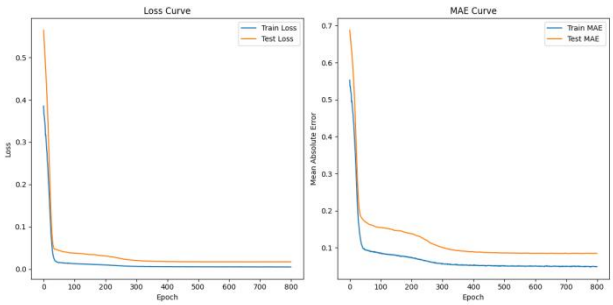

Figure 5. Training set and test set MSE and MAE curves

In this graph, the horizontal axis indicate the time period, and the vertical axis represents the model's mean square error and average absolute error. When the Epoch reaches 800 times, the loss rate converges well and eventually stabilizes at a value

around 0.011. This deformation prediction model has a relatively high prediction accuracy.

4.4 Predicted Results

The input layer of the LSTM model adopted has 5 nodes, the output layer has 1 node, the hidden layer has 10 nodes, and there is 1 fully connected layer (Hao et al., 2022). The delay step size is set to 10. After the parameter settings are completed, the cumulative deformation data obtained from feature points P1, P2, and P3 are used as the dataset. The dataset is split into two sets: a training set and a test set. The training set makes up 60% of the dataset, while the test set makes up 40%. Here, dividing the training set and test set in a 6:4 ratio can ensure that the model has sufficient data for training while also providing sufficient test data for predicting the cumulative deformation of feature points within the landslide area. Finally, the LSTM model prediction results for the cumulative deformation displacement of the 3 feature points in the landslide area are obtained, as shown in Figure 6.

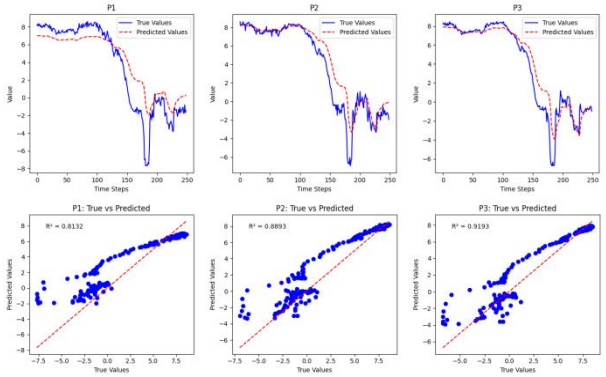

Figure 6. Test set LSTM accuracy evaluation index

As shown in Figure 6, the prediction results of the respective LSTM models for the characteristic points P1, P2, and P located on the surface of the slope body are consistent with the cumulative deformation trend of the actual values. Moreover, the goodness of fit (R^2) of each characteristic point within the sliding body area is greater than 0.80. This result indicates that the fitting degree between the predicted values and the actual values is relatively high (Table 3).

feature points	MAE	MSE	R^2
P1	1.23	0.96	0.81
P2	0.45	0.64	0.89
P3	0.21	0.30	0.92

Table 3. Evaluation indicators for LSTM accuracy of the test set

By comparing the absolute errors between the predicted values and the actual values of the three characteristic points on the slope surface, it can be seen that the absolute errors between the cumulative deformation prediction values calculated by the LSTM model for points P1, P2, and P3 and the actual values are all less than 6 mm. This result to some extent reflects the effectiveness of the cumulative deformation prediction results of the characteristic points obtained by using the LSTM model.

Furthermore, as can be seen from Figure 6 and Table 3, the goodness of fit (R^2) of P3 is 0.92, which is higher than that of P1 (0.81) and P2 (0.89). This indicates that the fitting degree between the predicted values and the actual values of P3 is higher than that of P1 and P2. The absolute error of the cumulative deformation result predicted by the LSTM model of P3 is smaller than that of P1 and P2. The value of P1 is relatively larger (Table 2), suggesting that the LSTM model performs better than P1 and P2 in predicting the cumulative deformation of P3.

5. Conclusion

This article uniquely blends the GB-InSAR technology and LSTM deep learning model, which suggests a highly accurate slope deformation narrowing and forecasting technology in open-pit mines. To begin with, the effect of time series deformation was monitored at the slope of a particular open-pit mine in Xilinhot, through the application of the GB-InSAR, which recorded time-series deformation at a high resolution, as well as providing a solid data base upon which future models could be built. Secondly, one LSTM prediction model of landslide deformation was built based on the deformation data collected to train and predict time series of the slope deformation pattern. Through the maximum use of the nonlinear sequential data processing capabilities of the LSTM network, the model features a high prediction accuracy, high robustness, and multi-scale feature extraction feature in the analysis of the complex deformation trends. The findings of the research are such that the proposed method may detect and track the landslide threats at an earlier phase, which introduces a novel research direction and efficient technical assistance to the safety control and prior warning of the open-pit mines slopes and reliable support of the active control and prevention of the geological disasters.

References

Chai, Z. H., Huang, J., Chen, L., Hao, F., & Wang, R. 2021. Sentiment analysis of e-commerce reviews based on long short-term memory networks with dropout layer and optimization. In 2021 20th international conference on ubiquitous computing and communications (IUCC/CIT/DSCI/SmartCNS) (pp. 369-374). IEEE.

Chang, L., Zhang, R., & Wang, C. 2022. Evaluation and prediction of landslide susceptibility in Yichang section of Yangtze River Basin based on integrated deep learning algorithm. Remote Sensing, 14(11), 2717.

Chataoui, J. 2024. Jointly-learnt exit and inference for dynamic neural networks. McGill University (Canada).

Chen, B., Li, W., Lu, H., Fu, H., Zhou, S., & Huang, W. 2024. Deformation Analysis of Jungong Ancient Landslide Based on SBAS-InSAR Technology in the Yellow River Mainstream. Geomatics and Information Science of Wuhan University, 49(8), 1407-1421.

Chen, Z., Huang, G., Xie, W., Zhang, Y., & Wang, L. 2023. GNSS Real-Time Warning Technology for Expansive Soil Landslide—A Case in Ningming Demonstration Area. Remote Sensing, 15(11), 2772. https://doi.org/10.3390/rs15112772

Cui, Y., Qian, Z., Xu, W., & Xu, C. 2024. A Small-Scale Landslide in 2023, Leshan, China: Basic Characteristics, Kinematic Process and Cause Analysis. Remote Sensing, 16(17), 3324.

Dai, Z., Zhang, Y., Zhang, C., Luo, J., & Yao, W. 2022. Interpreting the influence of reservoir water level fluctuation on the seepage and stability of an ancient landslide in the Three

Gorges Reservoir area: a case study of the Outang landslide. Geotechnical and Geological Engineering, 40(9), 4551-4561.

Gong, Y., Zhang, Y., Wang, F., & Lee, C. H. 2024. Deep learning for weather forecasting: A cnn-lstm hybrid model for predicting historical temperature data. arXiv preprint arXiv:2410.14963.

Han, J., Yang, H., Liu, Y., Lu, Z., Zeng, K., & Jiao, R. 2022. A deep learning application for deformation prediction from ground-based insar. Remote Sensing, 14(20), 5067.

Hao, G., Guo, J., Zhang, W., Chen, Y., & Yuen, D. A. 2022. High-precision chaotic radial basis function neural network model: Data forecasting for the Earth electromagnetic signal before a strong earthquake. Geoscience Frontiers, 13(1), 101315.

Huang, D., Kuang, X. B., & Luo, S. L. 2019. A study of the deformation characteristics and reactivation mechanism of the Outang landslide near the Three Gorges Reservoir of China. Hydrogeology & Engineering Geology, 46(5), 127-135.

Izumi, Y., Nico, G., & Sato, M. 2021. Time-series clustering methodology for estimating atmospheric phase screen in ground-based InSAR data. IEEE Transactions on Geoscience and Remote Sensing, 60, 1-9.

Izumi, Y., Zou, L., Kikuta, K., & Sato, M. 2020. Iterative atmospheric phase screen compensation for near-real-time ground-based InSAR measurements over a mountainous slope. IEEE Transactions on Geoscience and Remote Sensing, 58(8), 5955-5968.

Liu, Y., Xu, Q. J., Li, X. R., Yang, L. F., & Xu, H. 2023. Prediction of landslide block movement based on Kalman filtering data assimilation method. Journal of Mountain Science, 20(9), 2680-2691.

Liu, Y., Wang, W., Meng, X. et al. 2025. Hierarchical quantitative prediction of photovoltaic power generation depreciation expense based on matrix task prioritization considering uncertainty risk. Energy Inform 8, 8. https://doi.org/10.1186/s42162-024-00456-7

Li, Z., Lu, T., He, X., Montillet, J. P., & Tao, R. 2023. An improved cyclic multi model-eXtreme gradient boosting (CMM-XGBoost) forecasting algorithm on the GNSS vertical time series. Advances in Space Research, 71(1), 912-935.

Long, T. et al. 2022. Wideband Radar System Applications. In: Wideband Radar. Springer, Singapore. https://doi.org/10.1007/978-981-19-7561-5_6

Lv, W., Hu, X., Li, X., Zhao, J., Liu, C., Li, S., ... & Zhu, H. 2024. Multi-model comprehensive inversion of surface soil moisture from Landsat images based on machine learning algorithms. Sustainability, 16(9), 3509.

Ma, C., & Lu, B. 2023. Prediction of the Deformation of Heritage Building Communities under the Integration of Attention Mechanisms and SBAS Technology. Electronics, 12(23), 4724. https://doi.org/10.3390/electronics12234724

Song, X., Liu, Y., Xue, L., Wang, J., Zhang, J., Wang, J., ... & Cheng, Z. 2020. Time-series well performance prediction based on Long Short-Term Memory (LSTM) neural network model. Journal of Petroleum Science and Engineering, 186, 106682.

Wu, J., Chen, X. Y., Zhang, H., Xiong, L. D., Lei, H., & Deng, S. H. 2019. Hyperparameter optimization for machine learning models based on Bayesian optimization. Journal of Electronic Science and Technology, 17(1), 26-40.

Xiao, T., Huang, W., Deng, Y., Tian, W., & Sha, Y. 2021. Long-Term and Emergency Monitoring of Zhongbao Landslide Using Space-Borne and Ground-Based InSAR. Remote Sensing, 13(8), 1578. https://doi.org/10.3390/rs13081578

Xu, W., Lu, S., Lin, Z., & Zhou, W. 2025. Combination of InSAR and neural networks for the deformation monitoring and prediction of Fanjiaping landslide. Hydrogeology & Engineering Geology, 52(2), 150-163.

Yang, C., Zhang, T., Gao, G., et al. 2022. Application of SBAS-InSAR technology in monitoring of ground deformation of representative giant landslides in Jinsha river basin, Jiangda County, Tibet. The Chinese Journal of Geological Hazard and Control, 33(3), 94-105.

Yin, B., Yin, Y., Zhang, M., Zhang, C., He, Q., & Wang, G. 2024. Active fault control led to the Moli landslide triggered by rainfall on 26 February 2021 in Zhouqu County, Gansu, China. Landslides, 21(1), 83-98.

Zhang, R., Li, R., Liu, C., Zhu, J., & Shi, Y. 2025. Fault diagnosis method for wind turbine rolling bearings based on adaptive deep learning. Journal of Vibroengineering, 27(6), 957-977.

Zhang, P. H., & Zhou, Z. 2024. Vegetation distribution patterns and root mechanical properties of selected plant species on the Xijitan giant landslide in the upper reaches of the Yellow River. Acta Prataculturae Sinica, 33(1), 33.

Zhou, B., Peng, J. B., Yin, Y. P., Li, X., Wei, G., & Ma, X. 2014. Research on large-scale landslides between Lagan Gorge and Sigou Gorge in the upper reaches of Yellow River. Geological Review, 60(1), 138-143.

Zou, Z., Luo, T., Zhang, S., Duan, H., Li, S., Wang, J., ... & Wang, J. 2023. A novel method to evaluate the time-dependent stability of reservoir landslides: exemplified by Outang landslide in the Three Gorges Reservoir. Landslides, 20(8), 1731-1746.